Int. J. Electron. Commun. (AEÜ) xxx (2016) xxx–xxx

Contents lists available at ScienceDirect

International Journal of Electronics and Communications (AEÜ)

journal homepage: www.elsevier.com/locate/aeue

Regular Paper

Image deblurring and denoising by an improved variational model

Jianlou Xu [a,*], Aifen Feng [a], Yan Hao [a], Xuande Zhang [b], Yu Han [c]

[a] School of Mathematics and Statistics, Henan University of Science and Technology, Luoyang 471023, China
[b] School of Mathematics, Ningxia University, Yinchuan 750021, China
[c] College of Mathematic and Computational Science, Shenzhen University, Shenzhen 518060, China

A R T I C L E I N F O

Article history:
Received 19 June 2015
Accepted 16 May 2016
Available online xxxx

Keywords:
Total variation
Image denoising
Image deblurring
Staircase effect

A B S T R A C T

Total variation method has been widely used in image processing. However, it produces undesirable staircase effect. To alleviate the staircase effect, some fourth order variational models were studied, which lead to the restored images smoothing and some details lost. In this paper, a low-order variational model for image deblurring and denoising is proposed, which is based on the splitting technique for the regularizer. Different from the general split technique, the improved variational model adopts the L_1 norm. To compute the new model effectively, we employ an alternating iterative method for recovering images from the blurry and noisy observations. The iterative algorithm is based on decoupling of deblurring and denoising steps in the restoration process. In the deblurring step, an efficient fast transforms can be employed. In the denoising step, the primal–dual method can be adopted. The numerical experiments show that the new model can obtain better results than those by some recent methods.

1. Introduction

The problem of image restoration has been widely studied in the last several years. The goal of image restoration is to recover the true image f from the observed noisy image

$$u_0 = Hf + \eta, \tag{1}$$

where u_0 is the observed noisy image, H is a bounded linear operator representing the convolution, and η denotes the additive Gaussian white noise.

Recovering f from u_0 is a typical example of an inverse problem. Since inverse problems are typically ill posed, a classical way to overcome ill-posed minimization problems is to add some regularization terms to the energy. This idea was firstly introduced by Tikhonov and Arsenin [1] as follows:

$$\min_f \int_\Omega |Hf - u_0|^2 dx + \frac{\lambda}{2} \int_\Omega |\nabla f|^2 dx, \tag{2}$$

where $\lambda > 0$ is a regularization parameter which balances the first and second terms. However, this model has very strong isotropic smoothing properties and tends to make images overly smooth, it often fails to adequately preserve important image attributes such as sharp edges. In order to overcome these drawbacks, the authors in [2] used the Total Variation (TV) of f instead of the L_2 norm of the gradient of f and proposed the following model

$$\min_f \int_\Omega |Hf - u_0|^2 dx + \lambda \int_\Omega |\nabla f| dx. \tag{3}$$

Although the TV regularizer has the ability of preserving the edges, it also gives rise to some undesired effects and transforms smooth signal into piecewise constant, the so-called staircase effects. In order to reduce the staircase effect, some high-order variational models were introduced [3–8], which contain the second order TV regularization terms. However, those high-order variational models need more complex boundary conditions.

Due to the nondifferentiability and nonlinearity of the TV function, Eq. (3) is more difficult to solve, some fast algorithms sprang up in recent years [9–13]. The authors in [9] used the variable-splitting and penalty techniques to solve the model. Ref. [10] and Ref. [11] put to use majorization–minimization method and alternating direction method for the TV image deblurring problems. In addition, the authors in [12,13] further studied the total bounded variational models for image deblurring and denoising problems. Nikolova et al. [14] studied nonconvex nonsmooth minimization methods for image restoration. There are also other methods for image deblurring, such as kernel regression [15], soft-thresholding method [16,17], nonlocal method [18], and wavelet method [19], etc.

Recently, to overcome the nondifferentiability and nonlinearity of the TV function of f in Eq. (3), Huang, Ng and Wen [20] intro-

* Corresponding author.
E-mail address: xujianlou@126.com (J. Xu).

http://dx.doi.org/10.1016/j.aeue.2016.05.008
1434-8411/

duced a new auxiliary variable u and proposed a fast TV minimization method as follows:

$$\min_{f,u} \frac{1}{2}\|Hf-u_0\|_2^2+\frac{\lambda}{2}\|f-u\|_2^2+\alpha\int_\Omega |\nabla u|dx, \tag{4}$$

where λ, α are positive regularization parameters. With this new auxiliary variable u, Eq. (4) can be solved effectively by decoupling of deblurring and denoising steps in the restoration process. In the deblurring step, fast transforms can be employed. In the denoising step, the TV model is solved by dual algorithm. Because the TV regularization term in Eq. (4) produces the staircase effect, in order to reduce it, the authors in [4] used the second order TV of u instead of the first order TV of u in Eq. (4) to design the following model

$$\min_{f,u} \frac{1}{2}\|Hf-u_0\|_2^2+\frac{\lambda}{2}\|f-u\|_2^2+\alpha\int_\Omega |\nabla^2 u|dx. \tag{5}$$

With the above model (5), the authors provided better results. However, the high-order TV regularizer causes some edges and details smoothed out, which are the very important characteristics in the restored images.

Inspired by the splitting idea [20], we introduce an auxiliary variable in the regularization term of Eq. (5) and divide the second order derivative term into two low order terms. The aim is that it not only can lower the order of image, but can alleviate the staircase effect. To solve the proposed model effectively, we also design an alternating iterative algorithm. From the experimental results, we see that the new model obtains better results than some current state-of-the-art methods. In addition, the new model's order is lower than the fourth order, so it does not need the more complex boundary condition than the fourth order diffusion equations.

In the rest of this paper, we will give the new model in Section 2. In Section 3, we do some numerical experiments to test our algorithm. Finally, Section 4 concludes this paper.

2. The proposed model and algorithm

2.1. The proposed model

From Eq. (4), we can see that it in fact splits the regularization term f of Eq. (3) into two terms by introducing an auxiliary variable u. When λ goes to infinity, the solution of Eq. (4) converges to that of Eq. (3). By the variable splitting, the operator of gradient and the operator of convolution can be computed respectively, and Eq. (4) can be solved by some fast algorithms effectively. Inspired by this idea, we introduce a new auxiliary variable $\boldsymbol{v}$ and propose the following model

$$\min_{u,\boldsymbol{v},f} \frac{\beta}{2}\int_\Omega (Hf-u_0)^2dx \\ +\frac{\lambda}{2}\|f-u\|_2^2+\alpha_1\int_\Omega|\nabla u-\boldsymbol{v}|dx+\alpha_2\int_\Omega|\nabla\boldsymbol{v}|dx, \tag{6}$$

where β, λ, α_1, α_2 are the regularization parameters.

The proposed model has the following advantages: firstly, when $\alpha_1\to\infty$, then $\boldsymbol{v}=\nabla u$, and Eq. (6) turns into Eq. (5), that is, it contains the second order TV, so it can reduce the staircase effect. When $\alpha_2\to\infty$, then $\nabla\boldsymbol{v}\to 0$, the regularizer in Eq. (6) turns into the first order TV which is similar to Eq. (4), and it has the ability of preserving edges. All in all, Eq. (6) can automatically balance the first and second order terms by the parameters α_1,α_2, and it has the abilities of preserving the edges and reducing the staircase effect, which has been proved in [21,22].

Secondly, our variable splitting is different from Eq. (4) and [9]. We adopt the L_1 norm between vector $\boldsymbol{v}$ and the gradient of u not the L_2 norm. The advantage of this norm is that it can overcome the shortcoming of overly smooth, because the Euler–Lagrange of the L_2 norm produces the Laplace operator, which can smooth edges and details of the restored images.

From the above explanation, we can conclude that the proposed model provides a way of balancing between the first and second order of the objective function, so it can reduce the staircase effect while denoising. Meanwhile, it has the properties of edge preservation which is very important in image deblurring.

2.2. The proposed algorithm

To solve the proposed model (6), we use the following alternating direction method. The iterative algorithm is based on decoupling of denoising and deblurring steps in the image restoration process. It can be written into the following two minimization subproblems:

(1) Denoising step. For f fixed, find the solutions of $u,\boldsymbol{v}$

$$(u^{k+1},\boldsymbol{v}^{k+1})=\arg\min_{u,\boldsymbol{v}}\ \alpha_1\int_\Omega|\nabla u-\boldsymbol{v}|dx+\alpha_2\int_\Omega|\nabla\boldsymbol{v}|dx \\ +\frac{\lambda}{2}\|f^k-u\|_2^2. \tag{7}$$

(2) Deblurring step. For u fixed, find the solution of f

$$f^{k+1}=\arg\min_f\ \frac{\beta}{2}\|Hf-u_0\|_2^2+\frac{\lambda}{2}\|f-u^{k+1}\|_2^2. \tag{8}$$

We now give the corresponding algorithms for Eq. (7) and Eq. (8) respectively. First, for Eq. (7), by applying the Legendre–Fenchel transform, we obtain

$$\begin{aligned}&\arg\min_{u,\boldsymbol{v}}\ \alpha_1\int_\Omega|\nabla u-\boldsymbol{v}|dx+\alpha_2\int_\Omega|\nabla\boldsymbol{v}|dx+\frac{\lambda}{2}\|f^k-u\|_2^2\\ &=\arg\min_{u,\boldsymbol{v}}\ \max_{\boldsymbol{p}\in P,\boldsymbol{q}\in Q}\langle\nabla u-\boldsymbol{v},\quad \boldsymbol{p}\rangle+\langle\nabla\boldsymbol{v},\quad\boldsymbol{q}\rangle+\frac{\lambda}{2}\|f^k-u\|_2^2,\end{aligned} \tag{9}$$

where $P=\{\boldsymbol{p}=(p_1,p_2)^T\,|\,|\boldsymbol{p}|\leqslant\alpha_1\}$, $\quad Q=\left\{\boldsymbol{q}=\begin{pmatrix}q_{11}, & q_{12}\\ q_{21}, & q_{22}\end{pmatrix}\,|\,|\boldsymbol{q}|\leqslant\alpha_2\right\}$, $\boldsymbol{p}$, $\boldsymbol{q}$ are the dual variables.

Applying the primal–dual method in [21,23] to Eq. (9), we can get the iterative schemes as follows:

$$\begin{cases}\boldsymbol{p}^{k+1}=proj_P(\boldsymbol{p}^k+\delta(\nabla\bar{u}^k-\bar{\boldsymbol{v}}^k))\\ \boldsymbol{q}^{k+1}=proj_Q(\boldsymbol{q}^k+\delta(\nabla\bar{\boldsymbol{v}}^k))\\ u^{k+1}=\frac{u^k+\tau\lambda f^k+\tau div\,\boldsymbol{p}^{k+1}}{1+\tau\lambda}\\ \boldsymbol{v}^{k+1}=\boldsymbol{v}^k+\tau(\boldsymbol{p}^k+div^h\boldsymbol{q}^{k+1})\\ \bar{u}^{k+1}=2u^{k+1}-u^k\\ \bar{\boldsymbol{v}}^{k+1}=2\boldsymbol{v}^{k+1}-\boldsymbol{v}^k\end{cases} \tag{10}$$

where $proj_P(\tilde{\boldsymbol{p}})=\frac{\tilde{\boldsymbol{p}}}{\max(1,|\tilde{\boldsymbol{p}}|/\alpha_1)}$, $\quad proj_Q(\tilde{\boldsymbol{q}})=\frac{\tilde{\boldsymbol{q}}}{\max(1,|\tilde{\boldsymbol{q}}|/\alpha_2)}$ for any $\tilde{\boldsymbol{p}},\tilde{\boldsymbol{q}}$; δ,τ are positive parameters.

Second, for Eq. (8), its corresponding Euler–Lagrange equation is

$$\beta H^T(Hf^{k+1}-u_0)+\lambda(f^{k+1}-u^{k+1})=0, \tag{11}$$

so we have

$$(\lambda I+\beta H^TH)f^{k+1}=(\beta H^Tu_0+\lambda u^{k+1}). \tag{12}$$

Because of the regularized term λI, the coefficient matrix $(\lambda I+\beta H^TH)$ is always invertible. We can obtain a closed solution for Eq. (12) as follows.

$$f^{k+1}=(\lambda+\beta H^TH)^{-1}(\beta H^Tu_0+\lambda u^{k+1}). \tag{13}$$

We note that when some boundary conditions, such as periodic boundary conditions, zero boundary conditions, et al., are applied

Please cite this article in press as: Xu J et al. Image deblurring and denoising by an improved variational model. Int J Electron Commun (AEÜ) (2016), http://dx.doi.org/10.1016/j.aeue.2016.05.008

Table 1
The experimental results of four methods for different noise levels.

Image	Noise	[4]			[9]			[14]			Our		
		SNR	ReErr	SSIM	SNR	ReErr	SSIM	SNR	ReErr	SSIM	SNR	ReErr	SSIM
Barbara	0.01	10.540	0.0123	0.7414	10.454	0.0126	0.7434	10.586	0.0122	0.7354	10.713	0.0118	0.7401
	0.05	9.8034	0.0146	0.6586	9.5283	0.0155	0.6562	9.5496	0.0155	0.6376	9.7715	0.0147	0.6525
	0.1	9.2233	0.0167	0.6040	9.0077	0.0175	0.6063	8.9351	0.0178	0.5768	9.2168	0.0167	0.5996
	0.2	8.4084	0.0201	0.5489	8.2485	0.0209	0.5450	8.2165	0.0210	0.5274	8.4572	0.0199	0.5430
Boat	0.01	14.600	0.0040	0.9511	14.881	0.0037	0.9488	14.851	0.0038	0.9521	15.018	0.0036	0.9540
	0.05	12.350	0.0067	0.8659	12.471	0.0065	0.8717	12.198	0.0069	0.8705	12.471	0.0065	0.8665
	0.1	10.927	0.0093	0.7813	10.901	0.0093	0.8004	10.791	0.0096	0.7983	11.067	0.0090	0.7981
	0.2	9.0717	0.0142	0.6596	9.4727	0.0129	0.7078	9.2925	0.0135	0.7078	9.4950	0.0129	0.7049
Cameraman	0.01	13.650	0.0093	0.8323	14.224	0.0082	0.8260	14.492	0.0077	0.8371	14.499	0.0077	0.8417
	0.05	12.132	0.0132	0.7158	12.279	0.0128	0.7585	12.534	0.0121	0.7659	12.584	0.0119	0.7535
	0.1	11.027	0.0171	0.6612	11.087	0.0168	0.7223	11.388	0.0157	0.7083	11.560	0.0151	0.7098
	0.2	9.5648	0.0239	0.5308	9.9705	0.0218	0.6543	10.087	0.0212	0.6828	10.241	0.0204	0.6434
House	0.01	16.962	0.0020	0.8622	15.563	0.0028	0.8679	17.633	0.0017	0.8665	17.900	0.0016	0.8678
	0.05	14.507	0.0035	0.7875	13.754	0.0042	0.8035	14.801	0.0033	0.8168	15.123	0.0031	0.7873
	0.1	12.742	0.0053	0.7250	12.369	0.0058	0.7820	12.895	0.0051	0.7831	13.529	0.0044	0.7811
	0.2	10.150	0.0097	0.6604	10.522	0.0089	0.7162	11.024	0.0079	0.7405	11.329	0.0074	0.7194
Lady	0.01	21.555	0.0015	0.9235	19.675	0.0023	0.9270	21.738	0.0015	0.9182	22.190	0.0013	0.9213
	0.05	18.387	0.0031	0.8439	17.459	0.0039	0.8497	18.051	0.0034	0.8523	18.762	0.0029	0.8435
	0.1	16.330	0.0050	0.7664	16.049	0.0054	0.8237	16.071	0.0054	0.8092	16.728	0.0046	0.7842
	0.2	14.418	0.0078	0.7351	14.131	0.0084	0.7461	14.353	0.0080	0.7534	14.798	0.0072	0.7509
Lena	0.01	15.088	0.0068	0.8683	14.563	0.0077	0.8572	15.453	0.0062	0.8575	15.707	0.0059	0.8671
	0.05	12.839	0.0114	0.7815	12.647	0.0119	0.7893	12.743	0.0117	0.7746	13.261	0.0103	0.7857
	0.1	11.478	0.0156	0.7147	11.256	0.0164	0.7404	11.192	0.0167	0.7093	11.823	0.0144	0.732
	0.2	9.8757	0.0226	0.6618	9.7577	0.0232	0.6689	9.8212	0.0228	0.6624	10.197	0.021	0.668
Pepper	0.01	14.009	0.0062	0.894	11.957	0.01	0.8993	12.824	0.0082	0.8796	14.352	0.0058	0.8905
	0.05	11.851	0.0103	0.816	10.90	0.0128	0.8254	10.968	0.0126	0.8114	11.539	0.011	0.8231
	0.1	10.654	0.0135	0.7515	9.9661	0.0158	0.7868	9.8392	0.0163	0.7482	10.473	0.0141	0.7632
	0.2	9.1952	0.0189	0.6995	8.8349	0.0205	0.7148	8.7466	0.021	0.7076	9.1524	0.0191	0.719
Toys	0.01	17.221	0.0026	0.9287	15.406	0.0039	0.9311	16.887	0.0028	0.9211	17.465	0.0025	0.9273
	0.05	13.557	0.006	0.842	12.946	0.007	0.8714	13.456	0.0062	0.8545	13.837	0.0057	0.8459
	0.1	11.329	0.0101	0.7717	11.392	0.0099	0.8264	11.543	0.0096	0.8137	12.203	0.0083	0.8251
	0.2	9.2102	0.0164	0.7205	9.4366	0.0156	0.7711	9.6466	0.0149	0.7628	9.980	0.0138	0.7645

Table 2
The corresponding average values for four different noises in Table 1.

Noise	[4]			[9]			[14]			Our		
	SNR	ReErr	SSIM	SNR	ReErr	SSIM	SNR	ReErr	SSIM	SNR	ReErr	SSIM
0.01	15.453	0.0056	0.8751	14.59	0.0065	0.8751	15.558	0.0056	0.871	15.981	0.0053	0.8763
0.05	13.179	0.0086	0.7891	12.749	0.0095	0.8033	13.038	0.009	0.7981	13.418	0.0084	0.7953
0.1	11.714	0.0116	0.722	11.504	0.0121	0.7609	11.581	0.0121	0.7433	12.062	0.0108	0.7474
0.2	9.987	0.0168	0.6523	10.047	0.0166	0.6905	10.148	0.0164	0.6931	10.457	0.0151	0.6891

to the image boundary, the matrix H can be diagonalized by the discrete fast transform [19].

From the above discussion, the detail algorithm for the proposed model is as follows:

Algorithm. The iterative algorithm for the proposed model (6).

Initialization: $u^0,\ \bar{u}^0,\ \boldsymbol{v}^0,\ \bar{v}^0 = 0,\ \boldsymbol{p}^0, \boldsymbol{q}^0 = 0,\ k = 0$
Step 1: Compute $u^{k+1},\ \boldsymbol{v}^{k+1}$ by Eq. (10),
Step 2: Compute f^{k+1} by Eq. (13),
Until: A stopping criterion is satisfied; otherwise set $k = k + 1$ and return to **Step 1**.

3. Numerical experiments

To validate the deblurring and denoising performance of the proposed model, we test several images using our algorithm. All test images are normalized to be in [0,1] In addition, in order to measure the quality of the restored image, Signal to Noise Ratio (SNR) in decibels (db), the Relative Error (Re*Err*) and Structural Similarity (SSIM) [24] are employed, which are defined as follows respectively:

$$\mathrm{SNR} = 10\log_{10}\frac{\|f^0 - \mu_{f^0}\|_2^2}{\|f^0 - u^*\|_2^2}, \quad \mathrm{Re}Err = \frac{\|u^* - f^0\|_2^2}{\|f^0\|_2^2},$$

$$\mathrm{SSIM}(f^0, u^*) = \frac{4\sigma_{f^0 u^*}\mu_{u^*}\mu_{f^0}}{\left(\sigma_{u^*}^2 + \sigma_{f^0}^2\right)\left(\mu_{u^*}^2 + \mu_{f^0}^2\right)},$$

where u^* is the restored image, f^0 is the original clean image, $\sigma_{u^*},\ \sigma_{f^0}$ are the standard deviation of u^* and f^0, $\mu_{u^*},\ \mu_{f^0}$ are the mean value of u^* and f^0, $\sigma_{f^0 u^*}$ is the covariance of u^* and f^0. SSIM has been widely used to test the quality of the restored image, and the value is higher, the structural similarity is better.

In the following experiments, we compare the new model with the high-order model [4], total variational model [9], and the nonconvex model [14], respectively. The parameters in [9] and [14] have been recommended, and the parameters of [4] have to be

Table 3
The experimental results of four methods for different images.

Image	Case	[4]			[9]			[14]			Our		
		SNR	Re*Err*	SSIM	SNR	Re*Err*	SSIM	SNR	Re*Err*	SSIM	SNR	Re*Err*	SSIM
Barbara	i	15.82	0.004	0.885	15.24	0.004	0.901	16.15	0.003	0.893	16.77	0.003	0.895
	ii	9.049	0.017	0.590	8.763	0.019	0.586	8.694	0.019	0.557	9.052	0.017	0.587
	iii	8.056	0.022	0.517	7.880	0.023	0.526	7.819	0.023	0.502	8.109	0.022	0.519
Boat	i	17.11	0.002	0.973	17.22	0.002	0.977	17.20	0.002	0.977	17.43	0.002	0.977
	ii	10.15	0.011	0.764	10.02	0.011	0.760	9.965	0.012	0.767	10.28	0.011	0.757
	iii	8.283	0.017	0.611	8.508	0.016	0.638	8.370	0.017	0.652	8.540	0.016	0.640
Cameraman	i	16.44	0.005	0.868	17.02	0.004	0.892	17.86	0.004	0.885	17.82	0.004	0.873
	ii	10.24	0.020	0.672	10.27	0.020	0.699	10.54	0.019	0.698	10.75	0.018	0.667
	iii	8.657	0.029	0.570	9.054	0.027	0.596	9.128	0.026	0.653	9.190	0.026	0.593
House	i	19.66	0.001	0.895	16.73	0.002	0.898	19.72	0.001	0.893	20.04	0.001	0.894
	ii	12.21	0.006	0.746	11.51	0.007	0.767	11.96	0.006	0.755	12.49	0.006	0.736
	iii	9.196	0.012	0.629	9.404	0.012	0.666	9.714	0.011	0.708	9.865	0.01	0.648
Lady	i	24.13	0.001	0.943	20.73	0.002	0.944	24.18	0.001	0.940	24.54	0.001	0.943
	ii	15.53	0.006	0.795	15.32	0.006	0.813	15.32	0.006	0.774	16.22	0.005	0.791
	iii	13.23	0.01	0.704	13.03	0.011	0.692	13.26	0.01	0.721	13.62	0.009	0.698
Lena	i	17.57	0.004	0.913	16.37	0.005	0.911	17.79	0.004	0.906	18.09	0.003	0.910
	ii	10.73	0.019	0.703	10.45	0.02	0.712	10.43	0.02	0.686	11.13	0.017	0.707
	iii	8.743	0.029	0.585	8.810	0.029	0.618	8.747	0.029	0.618	9.159	0.027	0.619
Pepper	i	17.64	0.003	0.925	12.58	0.009	0.92	17.01	0.003	0.909	18.44	0.002	0.92
	ii	9.858	0.016	0.737	9.344	0.018	0.762	9.220	0.019	0.730	9.901	0.016	0.753
	iii	7.953	0.025	0.656	8.018	0.025	0.66	7.918	0.025	0.667	8.272	0.023	0.667
Toys	i	19.78	0.001	0.953	16.55	0.003	0.953	19.01	0.002	0.946	19.56	0.002	0.951
	ii	11.40	0.01	0.803	10.81	0.011	0.817	10.83	0.011	0.785	11.29	0.01	0.789
	iii	8.628	0.019	0.731	8.359	0.02	0.712	8.897	0.018	0.741	8.987	0.017	0.721

Table 4
The corresponding average values for the different cases in Table 3.

Case	[4]			[9]			[14]			Our		
	SNR	Re*Err*	SSIM	SNR	Re*Err*	SSIM	SNR	Re*Err*	SSIM	SNR	Re*Err*	SSIM
i	18.519	0.0026	0.9194	18.519	0.0026	0.9194	18.615	0.0025	0.9186	19.086	0.0023	0.9204
ii	11.146	0.0131	0.7262	10.811	0.014	0.7395	10.870	0.014	0.719	11.389	0.0125	0.7234
iii	9.0933	0.0204	0.6254	9.1329	0.0204	0.6385	9.2316	0.0199	0.6578	9.4678	0.0188	0.6381

(a)

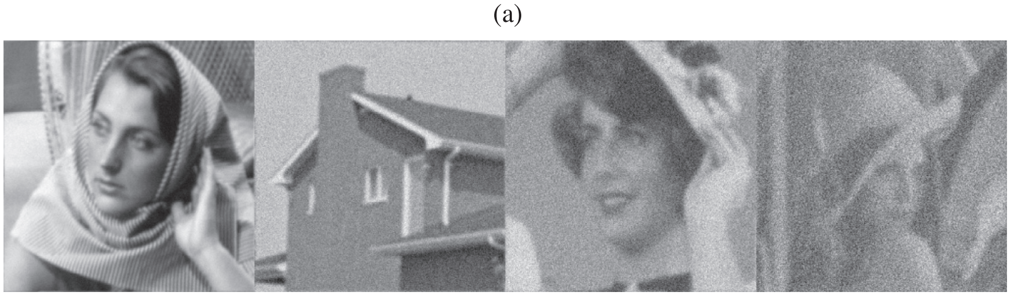

(b)

Fig. 1. Four clean and noisy images. (a) shows the clean images, and (b) shows the noisy and blurry images. From left to right, the noise is indicated by 0.01, 0.05, 0.1, 0.2, the corresponding supports are 5×5, 7×7, 9×9, 11×11 and σ are 1, 1.5, 2, 2.5, respectively.

Please cite this article in press as: Xu J et al. Image deblurring and denoising by an improved variational model. Int J Electron Commun (AEÜ) (2016), http://dx.doi.org/10.1016/j.aeue.2016.05.008

(a)

(b)

(c)

(d)

Fig. 2. Restoration results of different methods. From (a) to (d) the results are obtained by the recent model in [4], the model in [9], the model in [14] and the proposed model, respectively.

chosen by trial method. Note that the stopping condition in each algorithm is that it can obtain the best SNR values respectively.

We now give some parameters $\delta,\ \tau,\ \alpha_1,\ \alpha_2,\ \beta,\ \lambda$ to start up our algorithm. Firstly, parameters $\delta,\ \tau$ are used to control the convergence of algorithm. From [22], we know that the two parameters should be small as far as possible to guarantee algorithm to converge, however, if they are too small, the algorithm will be very slow, so in order to balance them, through some trials, we find that when $\delta \in [0.01, 1],\ \tau \in [0.01, 0.2]$, the proposed algorithm is very stable. So in the following experiments, we choose $\delta = 0.5$ and $\tau = 0.1$. For the parameters $\beta,\ \lambda$, it is important for us to choose the optimal values adaptively. Unfortunately, this problem has not been fully solved, and we have to choose them by the trial method. We test different values of $\beta,\ \lambda$ in order to find out the restored image with the highest SNR among the tested values and find that $\beta, \lambda \in [0.1, 0.5]$ are a relative good choice in the following experiments. $\alpha_1,\ \alpha_2$ are equilibrium parameters by manual adjustment according to different noise level. We observe that for 256×256 test images, when the noise level is 0.05, $\alpha_1, \alpha_2 \in [0.001, 0.1]$, the proposed algorithm can obtain good results. If the noise level is higher, take the bigger parameter α_1, we can obtain the better results.

We firstly test the performance of the proposed method under different levels of noise and the support is equal to 7×7. The tested Gaussian noises are with the standard deviation of 0.01, 0.05, 0.10 and 0.20, respectively. The tested blurring functions are chosen to be truncated two dimensional Gaussian function

$$h(s,t) = \exp\left(\frac{-s^2 - t^2}{2\sigma^2}\right), \quad -3 \leqslant s, t \leqslant 3, \tag{14}$$

with $\sigma = 1.5$. The experimental results are listed in Table 1. In order to evaluate the performances of different algorithms, we compute the respective average values for four noise levels in Table 2.

Secondly, we also test the following several conditions. (i) $\sigma = 1$ and the support is equal to 5×5 for the noise standard deviation 0.01; (ii) $\sigma = 2$ and the support is equal to 9×9 for the noise standard deviation 0.1; (iii) $\sigma = 2.5$ and the support is equal to 11×11 for the noise standard deviation 0.2. The corresponding results are listed in Table 3, and their respective average values in Table 4.

By inspection of Tables 1 and 2, we can observe that for most denoising results the proposed algorithm achieves better values of SNR, Re*Err* (SNR averagely exceed about 0.4db over the recent model in [4], 0.7 db over the model in [9], and over 0.4 db the model in [14]). For SSIM values, due to the use of the lower order TV regularizer, the proposed model averagely obtains higher SSIM values than the second order TV model in [4], which shows that the more details and edges are reserved. Even for the unsuccessful cases, our algorithm yields comparable value comparing with the best values. Consequently, we believe that the proposed model can averagely perform better than the other three models. Similarly, we get the similar results in Tables 3 and 4.

To make a visual comparison of the restoration images, we also give the restored results for four noise levels with four different images in Fig. 1. From the restored results in Fig. 2, we can see that the proposed model obtains the better visual resolution than other three methods.

4. Conclusions

A novel variational model for image deblurring and denoising is proposed, which is based on the splitting technique for the regularization term. Different from the general splitting technique, the improved variational model adopts the L_1 norm. In addition, we employ an alternating iterative method based on decoupling of deblurring and denoising steps in the restoration process. In the deblurring step, Fast Fourier Transform (FFT) is employed. In the denoising step, we use the primal–dual method. The numerical experiments show that the new model can obtain better results than those restored by some existing restoration methods.

Acknowledgments

This work is supported by the National Science Foundation of China (Nos. 61301229, U1504603, 61362029), the key scientific research project of Colleges and Universities in Henan Province (No. 15A110020), the soft science research project of Henan province (No. 142400411404) and the doctoral research fund of Henan University of Science and Technology (Nos. 09001708 and 09001751).

References

[1] Tikhonov A, Arsenin V. Solutions of ill-posed problems. Washington, DC: Winston and Sons; 1977.
[2] Rudin L, Osher S, Fatemi E. Nonlinear total variation based noise removal algorithms. Phys D 1992;60:259–68.
[3] Chan T, Marquina A, Mulet P. High-order total variation-based image restoration. SIAM J Sci Comput 2000;22(2):503–16.
[4] Lv X, Song Y, Wang S, et al. Image restoration with a high-order total variation minimization method. Appl Math Model 2013;37:8210–24.
[5] Lysaker M, Lundervold A, Tai X. Noise removal using fourth-order partial differential equation with applications to medical magnetic resonance images in space and time. IEEE Trans Image Process 2003;12(12):1579–90.
[6] Li F, Shen C, Fan J, et al. Image restoration combining a total variational filter and a fourth-order filter. J Vis Commun Image R 2007;18:322–30.
[7] Lysaker M, Tai X. Iterative image restoration combining total variation minimization and a second-order functional. Int J Comput Vis 2006;66(1):5–18.
[8] Liu G, Huang T, Liu J. High-order TVL1-based images restoration and spatially adapted regularization parameter selection. Comput Math Appl 2014;67:2015–26.
[9] Wang Y, Yang J, Yin W, et al. A new alternating minimization algorithm for total variation image reconstruction. SIAM J Imaging Sci 2008;1(3):248–72.
[10] Olivira J, Bioucas-Dias J, Figueiredo M. Adaptive total variation image deblurring: a majorization-minimization approach. Signal Processing 2009;89:1683–93.
[11] Wang S, Huang T, Liu J, et al. An alternating iterative algorithm for image deblurring and denoising problems. Commun Nonlinear Sci Numer Simul 2014;19:617–26.
[12] Liu X, Huang L. Split Bregman iteration algorithm for total bounded variation regularization based image deblurring. J Math Anal Appl 2010;372:486–95.
[13] Xu Y, Huang T, Liu J, et al. An augmented Lagrangian algorithm for total bounded variation regularization based image deblurring. J Franklin Inst 2014;351:3053–67.
[14] Nikolova M, Ng M, Tam C. Fast nonconvex nonsmooth minimization methods for image restoration and reconstruction. IEEE Trans Image Process 2010;19(12):3073–88.
[15] Takeda H, Farsiu S, Milanfar P. Deblurring using regularized locally adaptive kernel Regression. IEEE Trans Image Process 2008;17(4):550–63.
[16] Huang J, Huang T, Zhao X, et al. Two soft-thresholding based iterative algorithms for image deblurring. Inf Sci 2014;271:179–95.
[17] Beck A, Teboulle M. Fast gradient-based algorithms for constrained total variation image denoising and deblurring problems. IEEE Trans Image Process 2009;18(11):2419–34.
[18] Tang S, Gong W, Li W, et al. Non-blind image deblurring method by local and nonlocal total variation models. Signal Process 2014;94:339–49.
[19] Wen Y, Ng M, Ching W. Iterative algorithm based on decoupling of deblurring and denoising for image restoration. SIAM J Sci Comput 2008;30(5):2655–74.
[20] Huang Y, Ng M, Wen Y. A fast total variation minimization method for image restoration. SIAM Multiscale Model Simul 2008;7(2):774–95.
[21] Hao Y, Xu J, Bai J. Primal-dual method for the coupled variational model. Comput Electr Eng 2014;40:808–18.
[22] Hao Y, Xu J, Li S, et al. A variational model based on split Bregman method for multiplicative noise removal. AEU Int J Electron Commun 2015;69:1291–6. http://dx.doi.org/10.1016/j.aeue.2015.05.009.
[23] Chambolle A, Pock T. A first-order primal-dual algorithm for convex problems with applications to imaging. J Math Imaging Vision 2011;40(1):120–45.
[24] Wang Z, Bovik A, Sheikh H, et al. Image quality assessment: from error visibility to structural similarity. IEEE Trans Image Process 2004;13(4):1–14.

Please cite this article in press as: Xu J et al. Image deblurring and denoising by an improved variational model. Int J Electron Commun (AEÜ) (2016), http://dx.doi.org/10.1016/j.aeue.2016.05.008